Journal of Power Sources 224 (2013) 13–19

Contents lists available at SciVerse ScienceDirect

Journal of Power Sources

journal homepage: www.elsevier.com/locate/jpowsour

Preparation of 4.7 V cathode material $LiNi_{0.5}Mn_{1.5}O_4$ by an oxalic acid-pretreated solid-state method for lithium-ion secondary battery

Zhi Zhu [a], Hui Yan [a], Ding Zhang [b], Wei Li [c], Qi Lu [a,*]

[a] New Energy Materials and Technology Laboratory, Institute of Applied Chemistry, College of Chemistry and Molecular Engineering, Peking University, Beijing 100871, PR China
[b] Department of Applied Chemistry, College of Chemistry and Chemical Engineering, Taiyuan University of Technology, Taiyuan 030024, PR China
[c] School of materials science and engineering, University of Science and Technology Beijing, Beijing 100083, PR China

HIGHLIGHTS

- Cathode material $LiNi_{0.5}Mn_{1.5}O_4$ is obtained via a novel precursor treatment.
- Homogeneous ions distribution and controlled Mn valance state in the precursor.
- Superior cycling performance and 97.2% capacity above 4.7 V.
- Able to obtain satisfying rate performance by adjusting sintering temperature.

ARTICLE INFO

Article history:
Received 11 May 2012
Received in revised form
8 August 2012
Accepted 14 September 2012
Available online 27 September 2012

Keywords:
Lithium-ion secondary battery
High-voltage cathode material
Lithium nickel manganese oxides
Oxalate precursor

ABSTRACT

$LiNi_{0.5}Mn_{1.5}O_4$ as a 4.7 V cathode material is prepared through an oxalic acid-pretreated solid-state method. Oxalic acid is added to react with the mixture of $LiOH{\bullet}H_2O$, MnO_2 and $Ni(OH)_2$. This chemical pretreatment results in a sufficient mixing of Li, Ni and Mn ions in the precursor, and therefore promotes the generation of pure $LiNi_{0.5}Mn_{1.5}O_4$ in the following calcination even at a temperature as low as 500 °C. The material prepared at 750 °C has a highest crystallinity and a regular crystal shape with smoothly surface. Compared to traditional method, the $LiNi_{0.5}Mn_{1.5}O_4$ synthesized by this novel method shows much better electrochemical performances with an initial discharging capacity of 136.9 mAh g^{-1} and capacity retention of 93.4% after 300 cycles under 0.3C. And most importantly 97.2% of the total capacity displays at 4.7 V, which significantly favors the cell energy density. The novel preparation technique is also available to get high rate performance for $LiNi_{0.5}Mn_{1.5}O_4$. The material synthesized at 900 °C has a capacity of 121.2 mAh g^{-1} and stable cycling performance under 3C due to its lower polarization resistance.

1. Introduction

Amounts of researches focused on lithium-ion secondary batteries have demonstrated the critical roles of cathode materials in supplying high energy density and superior cycling performance [1–4]. Because of the privileges of low cost, non-toxicity and excellent thermal reliability, spinel $LiMn_2O_4$ has attracted intensive attentions among the various cathodes [4–7]. Despite this, a new generation of cathode material with higher voltage and energy density must be developed for the demands of future hybrid electrical vehicles (HEV) and electrical vehicles (EV) to travel more mileages. With the same spinel structure, $LiNi_{0.5}Mn_{1.5}O_4$ has a high voltage of 4.7 V, which means it can supply 30% extra voltage and energy density [8–13]. The distinct discharging voltage plateaus for the two spinels result from different redox reactions. In the process of charging and discharging, $Mn^{3+/4+}$ redox takes place in $LiMn_2O_4$ to make a 4.0 V discharging voltage, while $Ni^{2+/4+}$ redox carries out in $LiNi_{0.5}Mn_{1.5}O_4$ which makes the dominant voltage plateau around 4.7 V [14–16].

It is important to synthesize pure phase $LiNi_{0.5}Mn_{1.5}O_4$, for the presence of non-stoichiometric spinel will deteriorate its electrochemical performance [17]. Generally, $LiNi_{0.5}Mn_{1.5}O_4$ material can be synthesized by wet chemical method and solid-state method, which have been reviewed by Hagh [17] and Rambabu [18]. Typical wet chemical methods like sol-gel and co-precipitation can readily provide $LiNi_{0.5}Mn_{1.5}O_4$ with homogenous composition, narrow particle size distribution and a high discharge capacity above 135 mAh g^{-1} [19–24]. However, the $LiNi_{0.5}Mn_{1.5}O_4$ powders

* Corresponding author. Tel.: +86 10 62751000; fax: +86 10 62755290.
E-mail addresses: qilu@pku.edu.cn, tdg@pku.edu.cn (Q. Lu).

0378-7753/$ – see front matter © 2012 Elsevier B.V. All rights reserved.
http://dx.doi.org/10.1016/j.jpowsour.2012.09.043

prepared by these methods often have limited particle size. Thus, it results in a low tap density of the materials and the corresponding large cathode–electrolyte interface promotes some side reactions and in turns deteriorates its long term cycling stability [17]. Besides, it is noted that general wet chemical methods always require lots volumes of chemical solutions, rigorously controlled reacting temperature, pH and other complex operations to get homogenous precursors.

Solid-state method has a simple process and low cost to prepare massive $LiNi_{0.5}Mn_{1.5}O_4$ materials. Usually stoichiometric mixture of Li, Ni, Mn precursors is milled for 5–12 h, then sintered at 700–900 °C for 6–24 h [25,26]. The $LiNi_{0.5}Mn_{1.5}O_4$ obtained from $Ni(NO_3)_2 \cdot 6H_2O$ shows a highest initial capacity of 133 mAh g^{-1}, while the others are all below 120 mAh g^{-1} [26]. However, the material synthesized by traditional solid-state method often delivers an inferior cycling performance and notable capacity discharged near 4.0 V. Such $LiNi_{0.5}Mn_{1.5}O_4$ materials always contain impurity phases (such as $LiNiO_2$, NiO etc.) even if with repetition of high-energy ball-milling before sintering [2,10,27,28]. In addition, calcination at higher temperature will trigger another unwanted reaction (Eq. (1)) to introduce new mixed phases and oxygen loss [10,29]:

$$LiNi_{0.5}Mn_{1.5}O_4 \rightarrow qLi_zNi_{1-z}O + rLiNi_{0.5-w}Mn_{1.5+w}O_4 + sO_2 \quad (1)$$

To prepare pure $LiNi_{0.5}Mn_{1.5}O_4$ and investigate its property, here we have developed a novel solid-state method. Oxalic acid is added to the mixture of $LiOH\bullet H_2O$, MnO_2 and $Ni(OH)_2$. Such chemical treatment can achieve a sufficient uniform distribution of Li, Ni and Mn ions, as well as the well-controlled valance state of Mn. Thus it favors the generation of pure $LiNi_{0.5}Mn_{1.5}O_4$ spinel even at a lower temperature of 500 °C. For comparison, the $LiNi_{0.5}Mn_{1.5}O_4$ materials have also been synthesized by traditional solid-state method. Although oxalic acid has already been used to assist to prepare $LiNi_{0.5}Mn_{1.5}O_4$ in a few previous researches [30,31], to the best knowledge as we know, such strategy to prepare $LiNi_{0.5}Mn_{1.5}O_4$ in this paper and the as obtained superior electrochemical performances of it have not ever been reported. In addition, by adjusting the sintering temperature, $LiNi_{0.5}Mn_{1.5}O_4$ with high rate performance can also be obtained.

2. Experiments

2.1. Preparation of $LiNi_{0.5}Mn_{1.5}O_4$

In this work, $LiNi_{0.5}Mn_{1.5}O_4$ are synthesized by traditional solid-state method (named P1) and novel solid-state method (named P2), respectively. To synthesize P1, stoichiometric amount of $LiOH\bullet H_2O$, $Ni(OH)_2$ and MnO_2 are mixed in a ball-milling machine with anhydrous ethanol as dispersant for 1–2 h. Then the chemical mixture is preheated at 600 °C for 5 h followed by milling for another 1–2 h, and at last sintered at 700∼1000 °C for 12 h to obtain the final $LiNi_{0.5}Mn_{1.5}O_4$.

When synthesizing P2, stoichiometric amounts of $LiOH\bullet H_2O$, $Ni(OH)_2$ and MnO_2 (all the same chemicals with above) are mixed with 60–90 wt.% oxalic acid at room temperature. The mixture is stirred for 1 h to ensure a complete chemical reaction. Then the slurry is evaporated in vacuum condition below 50 °C and further dried at 110 °C for 0.5 h to get the precursor. Finally, the $LiNi_{0.5}Mn_{1.5}O_4$ was obtained by sintering the precursor at 500–900 °C for 6–8 h.

2.2. Material analysis

Powder X-ray diffraction measurement is carried out to identify the crystal structure of the obtained $LiNi_{0.5}Mn_{1.5}O_4$ materials on a Rigaku MutiFlex Diffractometer (D/max-2500, Japan) using Cu Kα-radiation at 20 kV and 4 mA. The scanning range of 2θ is from 10° to 90°. The surface micro-images of the obtained $LiNi_{0.5}Mn_{1.5}O_4$ powders are observed using a Scanning Electron Microscope (JEOL, JSM-5600LV, Japan) with an accelerating voltage of 20 kV. Thermal gravimetric analysis of the materials is performed with a TGA-DSC (Setaram Labsys, France) instrument, and the powders are heated at 10 °C min^{-1} in a constant air flow.

2.3. Electrochemical tests

CR2032 coin-type cells are utilized for electrochemical tests. The cells are fabricated of positive electrode which consists of 86 wt% $LiNi_{0.5}Mn_{1.5}O_4$ powder, 8 wt% carbon black and 6 wt% PVDF, Li metal sheet as negative electrode, polymer separator and liquid electrolyte. The separator is a micro-porous polypropylene membrane Celguard 2400, and the electrolyte solution is 1M $LiPF_6$ dissolved in a mixture of ethylene carbonate (EC), dimethyl carbonate (DMC) and ethyl methyl carbonate (EMC) with a volume ratio of 1:1:1. The cells are assembled in an argon protected glove box.

A LAND CT2001A 8-channel automatic battery test system (Wuhan Jinnuo Electronics Co., Ltd) is used to carry out constant current charging/discharging in a voltage range of 3.0–5.0 V. Cyclic voltammetry is performed on a CHI660D Electrochemical Workstation (Shanghai Chenhua Instruments Co., Ltd) over a sweep voltage range of 3.5–5.0 V to characterize the redox reactions of $LiNi_{0.5}Mn_{1.5}O_4$ cathodes during the electrochemical process.

3. Results and discussion

3.1. Thermal analysis

The reaction processes of traditional solid-state method and the novel process developed by us are discussed in this section.

The synthesis process of $LiNi_{0.5}Mn_{1.5}O_4$ material by traditional solid-state method is first reinvestigated by thermal gravimetric analysis. Fig. 1a shows the TG curve of heating the mixture of $LiOH\bullet H_2O$, MnO_2 and $Ni(OH)_2$ after ball-milling from 30 °C to 1000 °C. The mixture probably mutually reacts as listed in Table 1 to transform into $LiNi_{0.5}Mn_{1.5}O_4$.

In Fig. 1a, a continuous weight loss is observed from 270 °C to 700 °C on TG curve. It indicates that the main reactions to form $LiNi_{0.5}Mn_{1.5}O_4$ occur continually. And it further reveals that some obtained $LiNi_{0.5}Mn_{1.5}O_4$ might suffer from unneeded reaction time and thus decompose into impurity phase. From room temperature, the total mass loss in the experiment is 18.1%, much extent deviating from the theory value of 16.7%. In addition, the reactant mixture is often reported to be heated at above 800 °C to promote the atom diffusions. However, as is indicated on the TG curve, the obvious weight loss after 780 °C infers that some side reaction, possibly the decomposition of $LiNi_{0.5}Mn_{1.5}O_4$ carries out at such high temperature. Thus, it is difficult to synthesis pure $LiNi_{0.5}Mn_{1.5}O_4$ spinel by traditional solid-state method.

Fig. 1b is the TG curve of the obtained precursor in the novel synthesis method. The weight loss below 220 °C with small broad endothermic peak is attributed to the dehydration of mixed metal oxalate. The following immense weight loss on TG with an intense exothermic process between 285 and 320 °C is the decomposition of precursor. This synthesis mainly occurs in a narrow temperature scale near 300 °C, and the heat released from the exothermic spontaneous combustion possibly urges the generation of $LiNi_{0.5}Mn_{1.5}O_4$ spinel even below 500 °C. Besides, the total weight loss during the whole synthesis process is 46.3%, extremely close to the theory value of 46.1%.

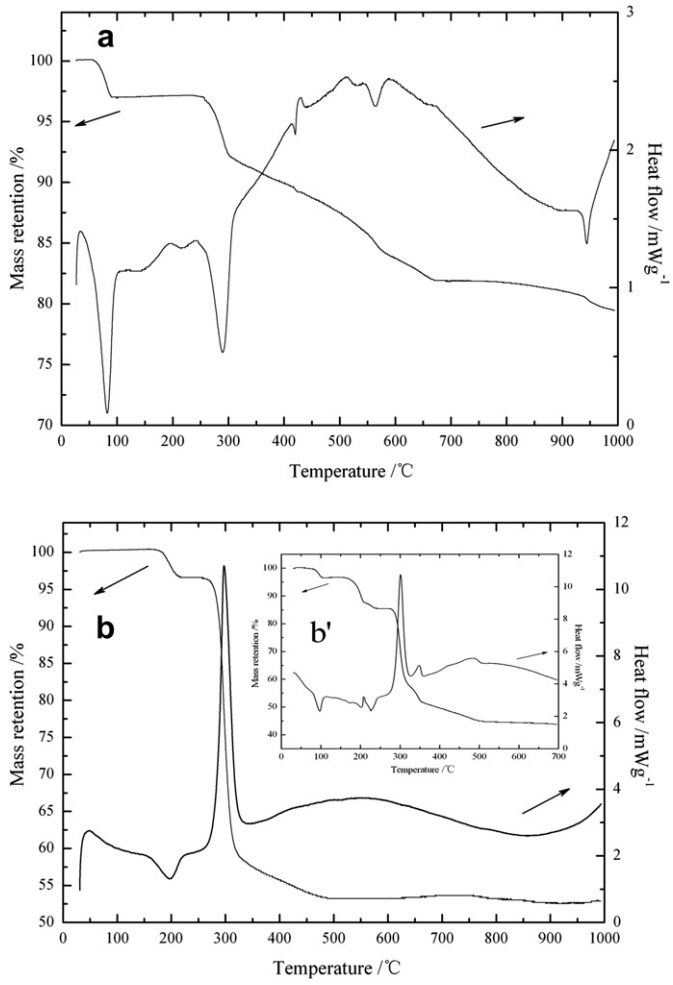

Fig. 1. TG curves of synthesizing $LiNi_{0.5}Mn_{1.5}O_4$ by (a) traditional solid-state method, (b) novel solid-state method from the obtained precursor, and (illustrated b') heating the mixture of lithium oxalate, nickel oxalate and manganese oxalate with 2:1:3 mole ratio.

In the chemical process to obtain the precursor, the oxalic acid easily reduces MnO_2 to Mn^{2+} and on another hand, it also participates the complexations with metallic ions to form composite oxalates. The curve in Fig. 1b', which is the TG curve of heating the mixture of lithium oxalate, nickel oxalate and manganese oxalate with a mole ratio of 2:1:3, has a different shape and exhibits obvious characteristic peaks of each oxalate and a total weight loss over 47.0%. Therefore it can be concluded that the obtained precursor in the novel method is not just a mechanical mixture of the three oxalates, but composed of Li, Mn and Ni ions uniformly distributed in atom scale and stoichiometric oxalic ions as sharing anion. The synthesis process in the novel method from raw mixtures can be revealed by Eq. (2) and Eq. (3)

Table 1
Possible reactions during sintering the raw mixture in traditional solid-state method.

Temperature	Reactions
Before 120 °C	$LiOH{\bullet}H_2O \rightarrow LiOH + H_2O$
During 270–700 °C	$Ni(OH)_2 \rightarrow NiO + H_2O$
	$LiOH(s) \rightarrow LiOH(l) \rightarrow Li_2O + H_2O$
	$Li_2O + NiO \rightarrow Li_2NiO_2$
	$4MnO_2 \rightarrow 2Mn_2O_3 + O_2$
	$Li_2O + NiO + 1.5Mn_2O_3 + 0.75O_2 \rightarrow 2LiNi_{0.5}Mn_{1.5}O_4$

$$2LiOH{\bullet}H_2O + Ni(OH)_2 + 3MnO_2 + 8H_2C_2O_4 \rightarrow Li_2NiMn_3{\cdot}5C_2O_4 + 12H_2O + 3CO_2 \quad (2)$$

$$Li_2NiMn_3{\cdot}5C_2O_4 + 4O_2 \rightarrow 2LiNi_{0.5}Mn_{1.5}O_4 + 10CO_2 \quad (3)$$

In the novel solid-state method, the chemical mixing process instead of mechanical ball-milling promotes the uniform distribution of Li, Ni and Mn ions at atom scale in the precursor. This will possibly ensure the feasibility of obtaining pure phase spinel at a lower temperature and in a shortened time. However, a weight loss of 1.6% is also observed at the temperature above 780 °C, that is, a decomposition of $LiNi_{0.5}Mn_{1.5}O_4$ also occurs at high temperature.

3.2. XRD and SEM analysis

XRD and SEM studies are performed to analysis the crystal structures and micro-images of the raw chemical, precursor and final products. Fig. 2a shows the X-Ray diffraction patterns of P1 synthesized at 700–1000 °C (named P1-700, 800, 900 and 1000, respectively). It indicates that they all have a spinel structure.

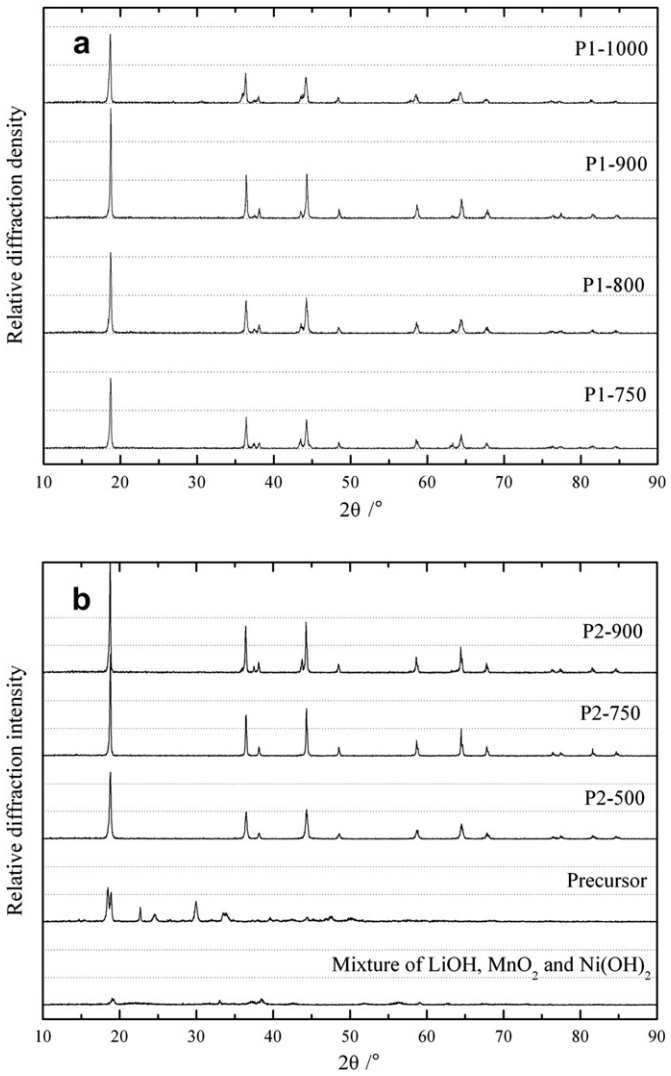

Fig. 2. XRD patterns of (a) $LiNi_{0.5}Mn_{1.5}O_4$ materials prepared by traditional solid-state method, and (b) the raw reactant mixture, precursor and resultant $LiNi_{0.5}Mn_{1.5}O_4$ by novel solid-state method, the dash line representing the same value of axis scale.

Meanwhile, obvious mixed phase diffraction peaks are observed on the XRD patterns near (311) and (400) peaks, but the intensity of that decreases with the increasing of sintering temperature until 900 °C. However, all the diffraction peaks weakens and broadens rapidly when the temperature continue increasingly to 1000 °C. This phenomenon may result from the serious decomposition of $LiNi_{0.5}Mn_{1.5}O_4$ above 900 °C (seen Eq. (1)).

Fig. 2b shows the XRD patterns of raw reactant mixture, precursor and resultant P2 products synthesized at 500 °C, 750 °C and 900 °C by the novel method. The raw mixture of $LiOH{\bullet}H_2O$, $Ni(OH)_2$ and MnO_2 has few crystal features, but characterize notable crystalline structure of oxalates after reacting with oxalic acid. A single phase spinel is obtained at a temperature as low as 500 °C, and the crystallinity is increased with the elevated sintering temperature. Compared with Fig. 2a, it suggests that both P2-750 and P2-900 have a higher crystallinity, though the appearance of impurity peaks near (311) and (400) is also observed when the $LiNi_{0.5}Mn_{1.5}O_4$ is synthesized at 900 °C.

The value of $I_{(311)}/I_{(400)}$ on XRD curve can be used somehow to measure the disordering degree of cation mixing which is always denoted as γ. γ can be calculated from the content of exchanged atom locations of lithium (8a) and manganese (16d) to form anti-spinel structure. Commonly, the value of $I_{(311)}/I_{(400)}$ increases with γ, along with a significant capacity fading [21,32]. In Fig. 2b, the $I_{(311)}/I_{(400)}$ value of P2-750 is 0.861, much lower than that of both P2-500 (0.944) and P2-900 (0.921). Thus, it can be expected that P2-750 will have a more stable cycling performance than P2-900.

The micro-images of raw reactant mixture, precursor and resultant products obtained at 750 °C and 900 °C by the novel solid-state method are shown in Fig. 3. It is clear that the mixture of $LiOH{\bullet}H_2O$, $Ni(OH)_2$ and MnO_2 has an amorphous morphology with wide distribution of particle sizes between 0.5 and 20 μm, but it converts to uniform sub-micrometer particles after the chemical reaction with oxalic acid. Fig. 3c suggests that the $LiNi_{0.5}Mn_{1.5}O_4$ particles observed at 750 °C has well-faceted crystallized octahedral morphology with particle size between 3 and 4 μm. The primary particles of the $LiNi_{0.5}Mn_{1.5}O_4$ spinel obtained at 900 °C, as shown in Fig. 3d, do not grow up in size anymore and turn to be a little agglomerated with a decomposed coarse surface.

3.3. Electrochemical performances

A $LiNi_{0.5}Mn_{1.5}O_4$ cell system versus Li metal as anode is designed and charged/discharged between 3.0 and 5.0 V with constant current to test the electrochemical performance of $LiNi_{0.5}Mn_{1.5}O_4$. Fig. 4 exhibits the charging and discharging curves of the obtained $LiNi_{0.5}Mn_{1.5}O_4$ under 0.3C, and the related data is listed in Table 2. It can be seen that most of the materials exhibit two plateaus during charging and discharging process: main capacity at 4.7 V attributed to $Ni^{2+/4+}$ redox couple, while a spot at 4.0 V based on $Mn^{3+/4+}$ redox couple.

From Fig. 4a, b and Table 2, P1-750 and P1-900 deliver an initial capacity of 112.9 mAh g^{-1} and 121.3 mAh g^{-1} respectively. And the cycling capacity retention is also maintained from 69.8% to 74.4% when the calcination temperature increased from 700 to 900 °C. It is clear that the capacity and cycling performance of $LiNi_{0.5}Mn_{1.5}O_4$ are apparently affected by the synthesis temperature in traditional solid-state method. A higher temperature is greatly required to improve the electrochemical performance of $LiNi_{0.5}Mn_{1.5}O_4$.

Synthesized by novel solid-state method, P2-750 has an initial capacity of 136.9 mAh g^{-1} and a capacity retention rate of 93.4% after 300 cycles; P2-900 shows that of 139.3 mAh g^{-1} and 78.8% (Fig. 4c, d and Table 2). Both of the capacity and cycling performance of P2 are greatly improved. The superior electrochemical performances of P2 ultimately attributed to the novel synthesis process. The uniform distribution of Li^+, Mn^{2+}, and Ni^{2+} in the precursor stimulates the generation of pure $LiNi_{0.5}Mn_{1.5}O_4$ spinel with high crystallinity and regular crystal morphology.

Additionally from Fig. 4 and Table 2, 97.2% of the capacity appears at 4.7 V high voltage for P2-750, while only 89.4% of that is for P2-900. The similar phenomenon has been reported that the

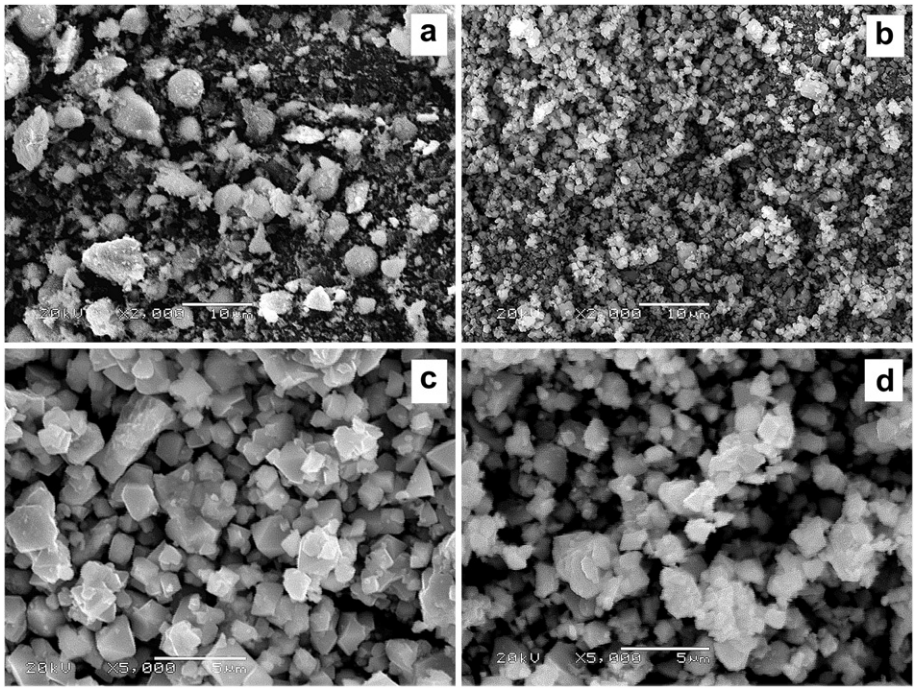

Fig. 3. SEM images of (a) the raw reactant mixture, (b) precursor and (c) resultant $LiNi_{0.5}Mn_{1.5}O_4$ materials obtained at 750 °C and (d) at 900 °C by the novel solid-state method.

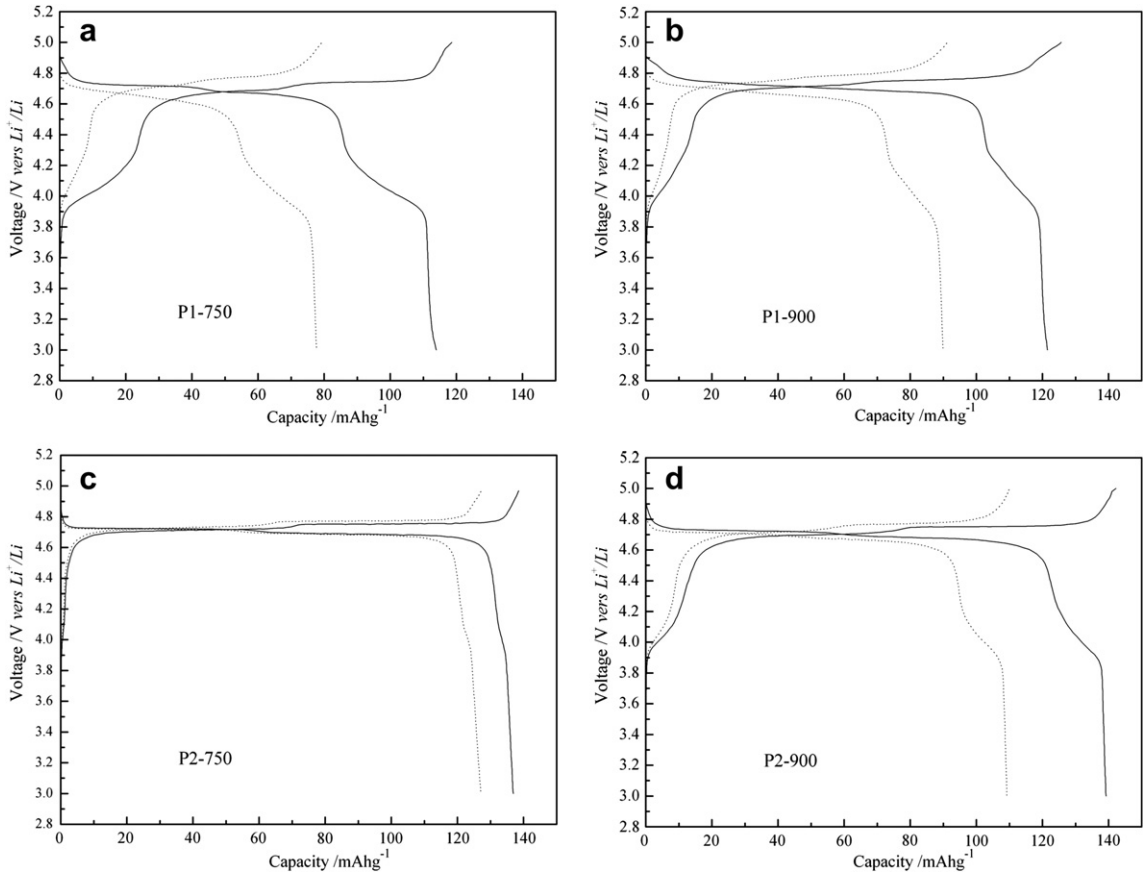

Fig. 4. Initial (solid line) and 300th (dash line) charging/discharging curves of $LiNi_{0.5}Mn_{1.5}O_4$ materials versus Li metal anode, with a constant current of 0.3C.

high calcination temperature leads to a reduction of Mn^{4+} to Mn^{3+}, and the yielded Mn^{3+}-O structure participates in the electrode redox reaction and in turn, results in the capacity at around 4.0 V [10,33,34]. Thus, synthesis at 750 °C efficiently avoids the spinel decomposition and the reduction of Mn^{4+}, resulting in a higher proportion of capacity at 4.7 V. Despite this, the capacity at 4.0 V low voltage of P2-900 has also been markedly restrained through the novel synthesis method compared to P1.

The result is well in agreement with the discussions on TG and XRD patterns (seen in Section 3.1 and 3.2). Among the obtained $LiNi_{0.5}Mn_{1.5}O_4$ materials, P2-750 has the highest capacity at 4.7 V high voltage and a highest capacity retention of 93.4% after 300 cycles under 0.3C. That is, the capacity fading is only about 0.03 mAh g^{-1} for each cycle.

In spite of the similar capacity delivered by P2-750 and P2-900 (Fig. 4c, d), the different proportion of that below 4.5 V will greatly influence the energy density of the battery. In actual application, energy is a more primary property of batteries than capacity, which directly determines the ability for energy storage of the batteries.

Table 2
Capacity and cycling retention of different $LiNi_{0.5}Mn_{1.5}O_4$, 0.3C.

Samples	Initial discharging capacity			Capacity after 300 cycles	
	3.0–5.0 V (mAh g^{-1})	4.5–5.0 V (mAh g^{-1})	Proportion above 4.5 V (%)	3.0–5.0 V (mAh g^{-1})	Cycling retention (%)
P1-750	112.9	84.7	75.0	78.8	69.8
P1-900	121.3	104.6	86.2	90.2	74.4
P2-750	136.9	133.1	97.2	127.9	93.4
P2-900	139.3	124.5	89.4	109.8	78.8

Thus in this research, a specific energy (E_s/mWh g^{-1}) is adopted to measure the $LiNi_{0.5}Mn_{1.5}O_4$ materials. Here E_s is defined as the energy furnished from unit mass of $LiNi_{0.5}Mn_{1.5}O_4$ active material with Li plate metal as anode. On the consideration of constant current discharging, the data of E_s can be obtained by the following equation:

$$E_s = \int P\,dt = \iint I\,dV\,dt = \int Q(V)\,dV \quad (4)$$

where P, I, t, V, and Q represent the discharging power (W), current (mA), length of time (h), voltage (V) and capacity (mAh g^{-1}), respectively. Therefore when discharged with a constant current, the specific energy released from the battery is directly determined by the discharging voltage scale.

Fig. 5 shows the energy releasing curves and energy cycling performances of the obtained $LiNi_{0.5}Mn_{1.5}O_4$. Synthesized through traditional solid-state method, P1-900 delivers an initial specific energy of 550 mWh g^{-1} when releasing to the prescribed minimum voltage of 3.0 V, and a retention less than 390 mWh g^{-1} after 300 cycles. Worse P1-750 releases an initial specific energy of only 518 mWh g^{-1} and just 332 mWh g^{-1} remains after 300 cycles. However, P2 samples perform much better and especially P2-750 has an initial specific energy as high as 644 mWh g^{-1} with a cycling retention of 592 mWh g^{-1} after 300 cycles. The much higher energy of P2-750 is not only attributed to the improved capacity, but to its higher percent of capacity at 4.7 V high voltage.

In addition, it is of great importance for the designed power batteries to supply a stable voltage, otherwise the decreased

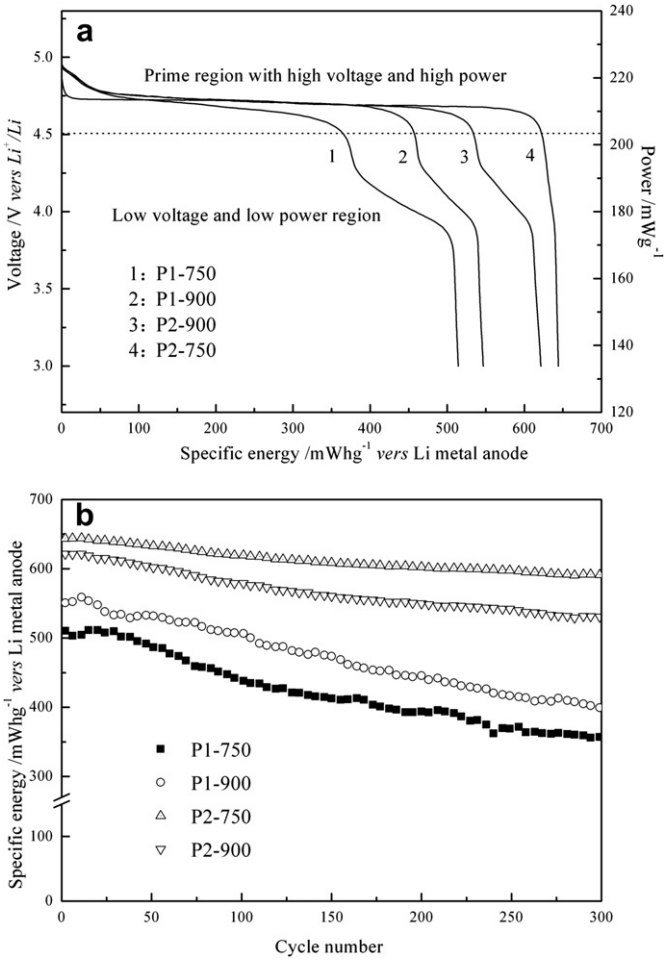

Fig. 5. Specific energy of $LiNi_{0.5}Mn_{1.5}O_4$ samples with Li metal as anode, (a) initial energy releasing curves, (b) energy cycling performance when releasing to 3.0 V with a constant current of 0.3C.

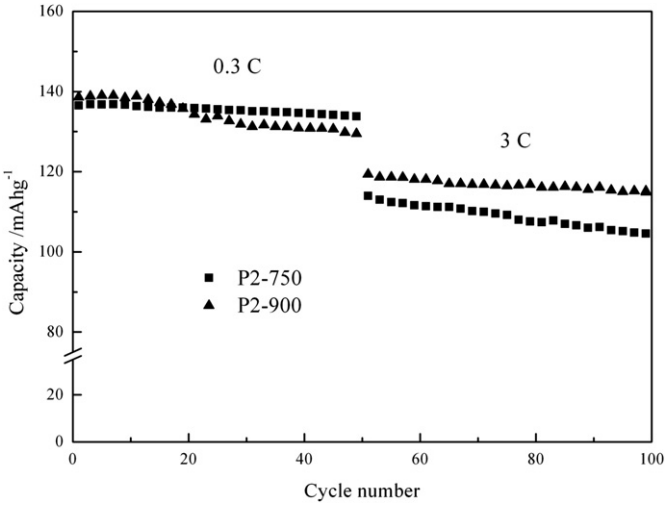

Fig. 6. Cycling performances of the obtained $LiNi_{0.5}Mn_{1.5}O_4$ under different rate currents.

voltage will not only loss much power but simultaneously bring in lots of harms to both motors and batteries. Therefore, the prime energy could be actually utilized of $LiNi_{0.5}Mn_{1.5}O_4$ is located above 4.6 V. From Fig. 5a, the prime energy of P2-750 reaches 634 mWh g^{-1}, which as far as known is the top value for that of $LiNi_{0.5}Mn_{1.5}O_4$ cathode material being reported among those prepared by solid-state method. The results indicate that synthesis at 750 °C by the novel process has not only increased the energy density of $LiNi_{0.5}Mn_{1.5}O_4$, but also made more percent of it released at a higher constant voltage and power.

Although P2-750 has higher capacity at 4.7 V and more stable cycling performance under 0.3C, the total initial capacity between 3.0 V and 5.0 V of P2-900 reaches 139.3 mAh g^{-1}, a little higher than that of P2-750. In addition, P2-750 and P2-900 are also charged and discharged under high rate current in this work, and Fig. 6 shows the cycling performance of them under 0.3C and 3C. It can be seen that though P2-750 has a more stable cycling performance under 0.3C, its capacity rapidly decreases to 114.2 mAh g^{-1} when cycled under 3C, and displays a serious attenuation in the following cycles. On the contrary, P2-900 displays a capacity of 121 mAh g^{-1} mAh g^{-1} and a much higher cycling retention than P2-750 under 3C.

To investigate the mechanisms resulting in the different electrochemical performances of P2-750 and P2-900, $LiNi_{0.5}Mn_{1.5}O_4$ cathodes is analyzed by cyclic voltammetry (CV) with a scanning rate of 0.1 mV s^{-1} from 3.5 V to 5.0 V. The value of ΔE ($|E_{ox} - E_{re}|$) between oxidation and reduction peaks corresponds to the polarization extent of the cathode material, as all the batteries are fabricated of the same system: using Li metal sheet as anode and $LiPF_6$ EC/DMC/EMC (1:1:1) as electrolyte.

Fig. 7 exhibits the CV performances of P2-750 and P2-900. It suggests that in the high-voltage region above 4.5 V, P2-750 displays two oxidation peaks at 4.73 V and 4.76 V, and one reduction peak at 4.69 V. The average ΔE for P2-750 is 55 mV. However, a slighter less ΔE of 21 mV is measured for P2-900, which shows double oxidation peaks at 4.71 V and 4.73 V, and double reduction peaks at 4.71 V and 4.69 V. It has been reported that the two oxidation peaks are attributed to the redox couples of Ni^{2+}/Ni^{3+} and Ni^{3+}/Ni^{4+} or the extrication of Li ions distributed at different locations in the structure [35–37]. It can be inferred that P2-900 delivers a more reversible redox behavior and lower polarization resistance in the beginning cycle. Therefore, it gives rise to a better high rate performance for P2-900.

However, it is also clear from Fig. 7 that after 300 cycles, the ΔE for P2-900 increases to 176 mV and on the CV curve, the double sharp redox peaks turn into one widen peak with asymmetry shape. It infers that a serious performance fading for P2-900 battery has taken place during the cycling process. On the other hand, the CV curve of P2-750 nearly keeps the same shape as the original curve. It demonstrates that $LiNi_{0.5}Mn_{1.5}O_4$ prepared at 750 °C significantly maintains the cathode interface stability, and consequently results in a stable cycling performance of P2-750 under 0.3C.

Additionally, another couple of redox peaks at 4.0 V can be clearly observed on the CV curve of P2-900, while no obvious peak is seen at the same region on P2-750. It suggests that P2-900 contains significant amount of Mn^{3+}, but that in P2-750 is negligible. Commonly, Mn^{3+} is considered unstable and inclines to decompose to Mn^{2+} and Mn^{4+}, whereas Mn^{2+} can dissolve into the electrolyte and along with Ni^{2+} cation, transports to anode through electrolyte and finally deposits on the surface of anode. As neither Mn^{2+} nor Ni^{2+} is helpful for the electrochemical performance, such metallic depositions result in the increases of interface impendence and capacity fading. However, the existence of some Mn^{3+} in the spinel also possibly favors the conductivity of $LiNi_{0.5}Mn_{1.5}O_4$ and can therefore improve the high rate performance of the material [24,38], as shown in Fig. 6.

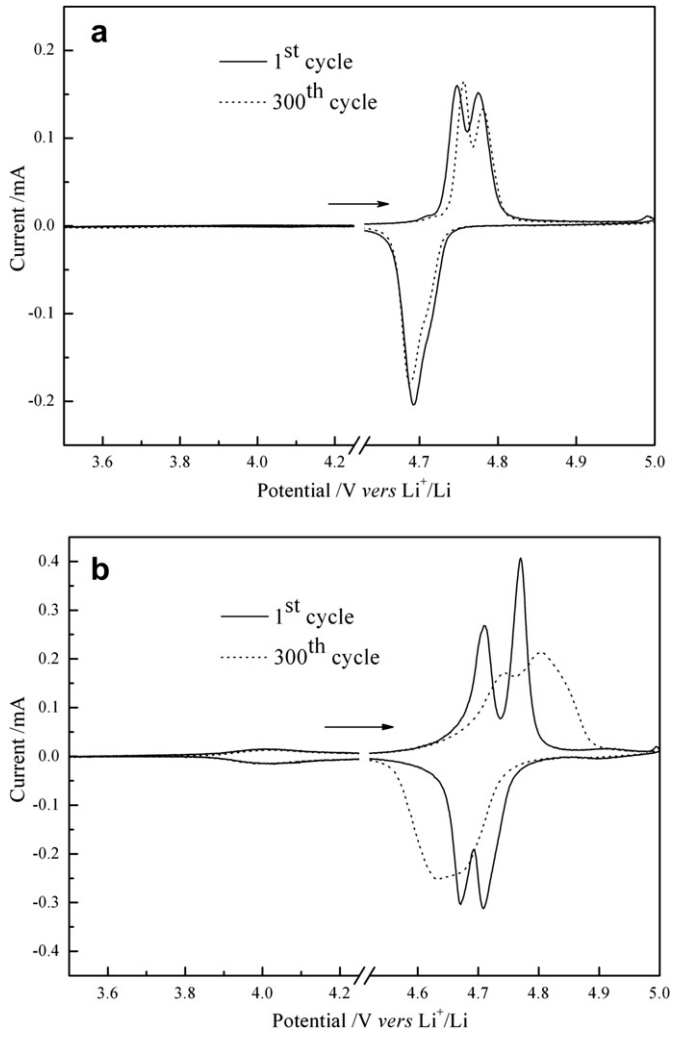

Fig. 7. Cyclic voltammetry curves of $LiNi_{0.5}Mn_{1.5}O_4$ synthesized by novel solid-state method at (a) 750 °C and (b) 900 °C, with a scanning rate of 0.1 mV s^{-1}.

4. Conclusion

A novel solid-state method has been developed to synthesis spinel $LiNi_{0.5}Mn_{1.5}O_4$ by chemically pretreating raw reactants to get a uniform precursor. The chemical mixing process promotes the formation of homogeneous precursor and hence enables the generation of product at 500 °C low temperature. The preparation of pure $LiNi_{0.5}Mn_{1.5}O_4$ spinel benefits from the following factors: On one hand, the high temperature synthesis proceeds sufficiently because of the well mixed metal-ions in the precursor; On another hand, calcination at 750 °C prevents the products from decomposition at higher temperature.

The novel method has not only simplified the complex process of traditional solid-state method, but at the same time improved the electrochemical performances of $LiNi_{0.5}Mn_{1.5}O_4$. And the intensive results show that the material synthesized at 750 °C delivers an initial capacity as high as 136.9 mAh g^{-1} with a retention of 93.4% after 300 cycles under 0.3C, and that synthesized at 900 °C had a capacity of 121.2 mAh g^{-1} and stable cycling performance under 3C. Furthermore, by releasing 97.2% of capacity at 4.7 V, the obtained $LiNi_{0.5}Mn_{1.5}O_4$ cathode has an energy density as high as 644 mWh g^{-1} (versus Li metal as anode).

Acknowledgment

This work is supported by National High Technology Research and Development Program of China (863) No. 2008AA11A102.

References

[1] T. Ohzuku, R.J. Brodd, Journal of Power Sources 174 (2007) 449–456.
[2] J.W. Fergus, Journal of Power Sources 195 (2010) 939–954.
[3] D. Guyomard, in: T. Osaka, M. Datta (Eds.), Energy Storage Systems for Electronics, New Trends in Electochemical Technology, vol. 1, Gordon and Breach, Amsterdam, 2000, pp. 253–350.
[4] M.S. Whittingham, Chemical Reviews 104 (2004) 4271–4301.
[5] S. Megahed, B. Scrosati, Journal of Power Sources 51 (1994) 79–104.
[6] J.M. Tarascon, B. Guyomard, Journal of the Electrochemical Society 138 (1991) 2864–2868.
[7] I. Belharouak, Y.K. Sun, W. Lu, K. Amine, Journal of the Electrochemical Society 154 (12) (2007) A1083–A1087.
[8] Q. Zhong, A. Bonakdarpour, M. Zhang, Y. Gao, J.R. Dahn, Journal of the Electrochemical Society 144 (1997) 205–213.
[9] T. Ohzuku, S. Takeda, M. Iwanaga, Journal of Power Sources 81–82 (1999) 90–94.
[10] K. Kanamura, W. Hoshikawa, T. Umegaki, Journal of the Electrochemical Society 149 (2002) A339–A345.
[11] S. Patoux, L. Daniel, C. Bourbon, H. Lignier, C. Pagano, F. Le Cras, S. Jouanneau, S. Martinet, Journal of Power Sources 189 (2009) 344–352.
[12] N.E. Sung, Y.K. Sun, S.K. Kim, M.S. Jang, Journal of Electrochemical Society 155 (11) (2008) A845–A850.
[13] K.M. Shaju, P.G. Bruce, Dalton Transactions 40 (2008) 5471–5475.
[14] Y. Terada, K. Yasaka, F. Nishikawa, T. Konishi, M. Yoshio, I.J. Nakai, Solid-State Chemistry 156 (2001) 286–291.
[15] M.Y. Song, D.S. Ahn, Solid State Ionics 112 (1-2) (1998) 21–24.
[16] J.H. Kim, S.T. Myung, Y.K. Sun, Electrochimica Acta 49 (2004) 219–227.
[17] R. Santhanam, B. Rambabu, Journal of Power Sources 195 (2010) 5442–5451.
[18] N.M. Hagh, G.G. Amatucci, Journal of Power Sources 195 (2010) 5005–5012.
[19] G.Q. Liu, Y.J. Wang, L. Qi, L. Wen, H. Chen, Electrochimica Acta 50 (9) (2005) 1965–1968.
[20] B.J. Hwang, Y.W. Wu, M. Venkateswarlu, M.Y. Cheng, R. Santhanam, Journal of Power Sources 193 (2009) 828–833.
[21] Y.S. Lee, Y.K. Sun, S. Ota, T. Miyashita, M. Yoshio, Electrochemistry Communications 4 (2002) 989–994.
[22] Y. Fan, J. Wang, X. Ye, J. Zhang, Materials Chemistry and Physics 103 (2007) 19–23.
[23] Y.K. Sun, S.W. Oh, C.S. Yoon, H.J. Bang, J. Prakash, Journal of Power Sources 161 (2006) 19–26.
[24] X. Fang, N. Ding, X.Y. Feng, Y. Lu, C.H. Chen, Electrochimica Acta 54 (2009) 7471–7475.
[25] Z. Chen, H. Zhu, S. Ji, V. Linkov, J. Zhang, W. Zhu, Journal of Power Sources 189 (2009) 507–510.
[26] H.S. Fang, Z.X. Wang, X.H. Li, H.J. Guo, W.J. Peng, Journal of Power Sources 153 (2006) 174–176.
[27] K. Takahashi, M. Saitoh, M. Sano, M. Fujita, K. Kifune, Journal of the Electrochemical Society 151 (1) (2004) A173–A177.
[28] S. Wu, S. Kim, Journal of Power Sources 109 (2002) 53–57.
[29] S.B. Park, W.S. Eom, W.I. Cho, H. Jang, Journal of Power Sources 159 (2006) 679–684.
[30] H.S. Fang, L.P. Li, G.S. Li, Journal of Power Sources 167 (2007) 223–227.
[31] T. Li, W.H. Qiu, G.H. Zhang, H.L. Zhao, J.J. Liu, Journal of Power Sources 174 (2007) 515–518.
[32] T. Ohzuku, K. Ariyoshi, S. Takeda, Y. Sakai, Electrochimica Acta 46 (2001) 2327–2336.
[33] Y. Idemoto, H. Narai, N. Koura, Journal of Power Sources 119–121 (2003) 125–129.
[34] C. Sigala, A. Le Gal La Salle, Y. Piffard, D. Guyomard, Journal of the Electrochemical Society 148 (2001) A826–A832.
[35] A.V. Ven, G. Ceder, Physical Reviews B 59 (1999) 742–749.
[36] A.V. Ven, C. Marianetti, D. Morgan, G. Ceder, Solid State Ionics 135 (2000) 21–32.
[37] J.H. Kim, S.T. Myung, C.S. Yoon, S.G. Kang, Y.K. Sun, Chemistry of Materials 16 (2004) 906–914.
[38] Y. Talyosef, B. Markovsky, G. Salitra, D. Aurbach, H.J. Kim, S. Choi, Journal of Power Sources 146 (2005) 664–669.